ANTICANCER RESEARCH *39*: 6489-6498 (2019)
doi:10.21873/anticanres.13863

Quantitative Structure–Cytotoxicity Relationship of 2-Styrylchromones

YOSHIHIRO UESAWA[1], JUNKO NAGAI[1], HAIXIA SHI[2,3], HIROSHI SAKAGAMI[3], KENJIRO BANDOW[4], AKITO TOMOMURA[4], MINEKO TOMOMURA[5], SAKI ENDO[6], KOICHI TAKAO[6] and YOSHIAKI SUGITA[6]

[1]*Department of Medical Molecular Informatics, Meiji Pharmaceutical University, Tokyo, Japan;*
[2]*Shanghai Ninth People's Hospital, Shanghai Jiatong University School of Medicine, Shanghai, P.R. China;*
[3]*Meikai University Research Institute of Odontology, Saitama, Japan;*
[4]*Division of Biochemistry, Meikai University School of Dentistry, Saitama, Japan;*
[5]*Department of Oral Health Sciences, Meikai University, Chiba, Japan;*
[6]*Department of Pharmaceutical Sciences, Faculty of Pharmacy and Pharmaceutical Sciences, Josai University, Saitama, Japan*

Abstract. *Background/Aim: Studies of biological activity of 2-styrylchromone derivatives focusing on antioxidant, anti-inflammatory, antiviral and antitumor activity are limited. In this study, eighteen synthetic 2-styrylchromone derivatives were investigated for their cytotoxicity against human malignant and non-malignant cells, and then subjected to quantitative structure–activity relationship (QSAR) analysis. Materials and Methods: Tumor-specificity was calculated by the ratio of mean 50% cytotoxic concentration (CC_{50}) against four normal oral cells to that against oral squamous cell carcinoma cell lines. Induction of apoptosis and growth arrest were evaluated by cell-cycle analysis. For QSAR analysis, 3,117 types of physicochemical, structural, and quantum chemical features were calculated from the most stabilized structure of 2-styrylchromone derivatives. Results: Two 2-styrylchromone derivatives in which a methoxy group was introduced at the 4-position of the benzene ring showed tumor-specificity equivalent to or higher than doxorubicin in TS value. These compounds accumulated the subG_1 and G_2/M phase cells, suggesting the induction of apoptosis. Their tumor-specificity can be explained mainly by molecular shape and electronic state. Conclusion: These findings suggest the applicability of 2-styrylchromone to develop safe and effective anticancer agents as seed compounds.*

Correspondence to: Yoshihiro Uesawa, Department of Medical Molecular Informatics, Meiji Pharmaceutical University, 2-522-1 Noshio, Kiyose, Tokyo 204-858, Japan. Tel: +81 424958892, e-mail: uesawa@my-pharm.ac.jp

Key Words: 2-Styrylchromones, cytotoxicity, tumor-specificity, QSAR analysis, cell cycle analysis, molecular shape.

Our group recently found that low-molecular weight natural polyphenols, such as tannins and flavonoids showed very low anticancer activity (evaluated by tumor-specificity with human cultured malignant and none-malignant cells) (1). On the other hand, chemical modification of chromone, two ring back-bone structure present in flavonoids, yielded derivatives with much higher tumor-specificity (2, 3).

2-Styrylchromone is a derivative having a styryl group bonded to the 2-position of the chromone skeleton. Synthetic 2-styrylchromone derivatives have been reported to show radical scavenging (4, 5), anti-inflammatory (6), hepatoprotective (7), neuroprotective (8-10), anti-human immunodeficiency virus (11), anti-norovirus (12), anti-rhinovirus (13, 14), antitumor (15-18), and monoamine oxidase B inhibiting (19) activity. However, very few studies tested their cytotoxicity against normal cells (16).

In the present study, we investigated the cytotoxicity of eighteen synthetic 2-styrylchromone derivatives (Figure 1) against four human oral squamous cell carcinoma (OSCC) cells lines (Ca9-22, HSC-2, HSC-3, HSC-4) and three human normal oral mesenchymal cells [human gingival fibroblast (HGF), human periodontal ligamental fibroblast (HPLF) and human pulp cell (HPC)], and performed quantitative structure–activity relationship (QSAR) analysis.

Materials and Methods

Materials. Dulbecco's modified Eagle's medium (DMEM) was purchased from GIBCO BRL (Grand Island, NY, USA); fetal bovine serum (FBS), doxorubicin, 3-(4,5-dimethylthiazol-2-yl)-2,5-diphenyltetrazolium bromide (MTT), ribonuclease (RNase) A from Sigma-Aldrich Inc. (St. Louis, MO, USA); dimethyl sulfoxide (DMSO), actinomycin D (FUJIFILM Wako Chem., Osaka, Japan); 100 mm dishes from True Line (Nippon Genetics Co., Ltd., Tokyo, Japan) and 96-well plates from TPP (Techno Plastic Products AG, Trasadingen, Switzerland).

Synthesis of test compounds. 2-[(1*E*)-2-Phenylethenyl]-4*H*-1-benzopyran-4-one [**1**], 2-[(1*E*)-2-(4-fluorophenyl)ethenyl]-4*H*-1-benzopyran-4-one [**2**], 2-[(1*E*)-2-(4-chlorophenyl)ethenyl]-4*H*-1-benzopyran-4-one [**3**], 2-[(1*E*)-2-(4-bromophenyl)ethenyl]-4*H*-1-benzopyran-4-one [**4**], 2-[(1*E*)-2-(4-methoxyphenyl)ethenyl]-4*H*-1-benzopyran-4-one [**5**], 2-[(1*E*)-2-(3,4-dimethoxy)ethenyl]-4*H*-1-benzopyran-4-one [**6**], 6-methoxy-2-[(1*E*)-2-phenylethenyl]-4*H*-1-benzopyran-4-one [**7**], 2-[(1*E*)-2-(4-fluorophenyl)ethenyl]-6-methoxy-4*H*-1-benzopyran-4-one [**8**], 2-[(1*E*)-2-(4-chlorophenyl)ethenyl]-6-methoxy-4*H*-1-benzopyran-4-one [**9**], 2-[(1*E*)-2-(4-bromophenyl) ethenyl]-6-methoxy-4*H*-1-benzopyran-4-one [**10**], 6-methoxy-2-[(1*E*)-2-(4-methoxyphenyl)ethenyl]-4*H*-1-benzopyran-4-one [**11**], 2-[(1*E*)-2-(3,4-dimethoxy)ethenyl]-6-methoxy-4*H*-1-benzopyran-4-one [**12**], 7-methoxy-2-[(1*E*)-2-phenylethenyl]-4*H*-1-benzopyran-4-one [**13**], 2-[(1*E*)-2-(4-fluorophenyl)ethenyl]-7-methoxy-4*H*-1-benzopyran-4-one [**14**], 2-[(1*E*)-2-(4-chlorophenyl)ethenyl]-7-methoxy-4*H*-1-benzopyran-4-one [**15**], 2-[(1*E*)-2-(4-bromophenyl)ethenyl]-7-methoxy-4*H*-1-benzopyran-4-one [**16**], 7-methoxy-2-[(1*E*)-2-(4-methoxyphenyl) ethenyl]-4*H*-1-benzopyran-4-one [**17**], and 2-[(1*E*)-2-(3,4-dimethoxy) ethenyl]-7-methoxy-4*H*-1-benzopyran-4-one [**18**] were synthesized by the condensation of the corresponding 2-methylchromones with selected benzaldehyde derivatives, according to previous methods (19). All compounds were dissolved in DMSO at 40 mM and stored at –20˚C before use.

Cell culture. Human OSCC cell lines (Ca9-22, derived from gingival tissue; HSC-2, HSC-3. HSC-4, derived from tongue) and human normal oral mesenchymal cells (HGF, HPLF, HPC) at 10-18 population doubling levels were cultured at 37˚C in DMEM supplemented with 10% heat-inactivated FBS, 100 units/ml, penicillin G and 100 μg/ml streptomycin sulfate under a humidified 5% CO_2 atmosphere, as described previously (20, 21).

Assay for cytotoxic activity. Cells were inoculated at 6×10^3 cells/cm^2 in a 96-microwell plate. After 48 h, the medium was replaced with fresh medium containing $(1/2)^2$ serially diluted test compounds. Cells were incubated for 48 h and the relative viable cell number was then determined in triplicate by MTT method, as described previously (20, 21). Control cells were treated with the same amounts of DMSO and the cell damage induced by DMSO was subtracted. The concentration of compound that reduced the viable cell number by 50% (CC_{50}) was determined from the dose–response curve.

Calculation of tumor-specificity index (TS). TS was calculated by the following equation: TS=Mean CC_{50} (HGF + HPLF + HPC)/ meanCC_{50} (Ca9-22 + HSC-2 + HSC-3 + HSC-4) (D/B) or CC_{50} (HGF)/C_{50} (Ca9-22) [both derived from gingival tissue (22)] (C/A in Table I), as described previously (20, 21).

Calculation of potency-selectivity expression (PSE). PSE, that is the product of tumor-specificity and cytotoxicity against tumor cells, was calculated by the following equation: PSE={Mean CC_{50} (normal cells)/[mean CC_{50} (OSCC cell lines)]^2}×100 [as shown in (D/B^2) ×100 or (C/A^2) ×100] (Table I) (20, 21).

Cell-cycle analysis. Treated and untreated cells (approximately 10^6 cells) were harvested from 100 mm dish, fixed with paraformaldehyde and then treated with ribonuclease A. After staining with propidium iodide in the presence of 0.01% Nonidet-40, filtering through cell strainers and the stained cells were subjected to cell sorting (SH800 Series; SONY Imaging Products and Solutions Inc., Kanagawa, Japan) and cell-cycle analysis with Cell Sorter Software version 2.1.2. (SONY Imaging Products and Solution Inc.), as described previously (21).

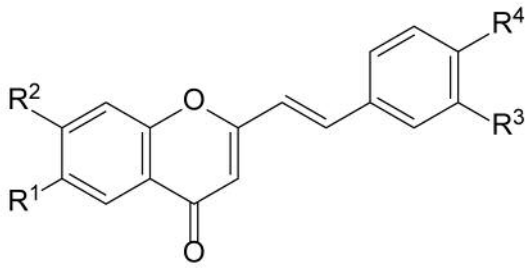

Compound	R^1	R^2	R^3	R^4
1	H	H	H	H
2	H	H	H	F
3	H	H	H	Cl
4	H	H	H	Br
5	H	H	H	OMe
6	H	H	OMe	OMe
7	OMe	H	H	H
8	OMe	H	H	F
9	OMe	H	H	Cl
10	OMe	H	H	Br
11	OMe	H	H	OMe
12	OMe	H	OMe	OMe
13	H	OMe	H	H
14	H	OMe	H	F
15	H	OMe	H	Cl
16	H	OMe	H	Br
17	H	OMe	H	OMe
18	H	OMe	OMe	OMe

Figure 1. *Structure of eighteen 2-styrylchromone derivatives **[1-18]** investigated in this study.*

Estimation of CC_{50} values for computational analysis. The negative log CC_{50} (pCC_{50}) values were used for the comparison of cytotoxicity between compounds, as described previously (21). The mean pCC_{50} values for normal cells and tumor cell lines were defined as N and T, respectively. The difference (T–N) was used as a tumor-specificity index in the following analyses (21).

Calculation of chemical descriptors. The 3D structure of each chemical structure (MarvinSketch 18.10.0, ChemAxon, Budapest,

Table I. *Cytotoxic activity of eighteen 2-styrylchromone derivatives [**1-18**] against oral malignant and non-malignant cells. Each value represents the mean of triplicate determinations. Two sets of tumor-specificity index (TS) and potency-selectivity expression (PSE) values were determined using human oral squamous cell carcinoma (OSCC) cell lines compared to human normal oral mesenchymal cells, and paired cells derived from the same (gingival) tissue.*

	CC_{50} (μM)														
	Human oral squamous cell carcinoma cell lines						Human normal oral cells								
	Ca9-22 A	HSC-2	HSC-3	HSC-4	Mean B	SD	HGF C	HPLF	HPC	Mean D	SD	TS D/B	TS C/A	PSE (D/B^2) ×100	PSE (C/A^2) ×100
1	23.3	57.0	46.0	24.3	37.7	16.6	79.7	109.3	48.7	79.2	30.3	2.1	3.4	5.6	14.7
2	28.5	13.0	33.7	3.9	19.8	13.8	264.0	248.7	14.0	175.6	140.1	8.9	9.3	44.9	32.4
3	8.6	6.3	11.4	16.0	10.6	4.2	281.0	333.0	40.3	218.1	156.1	20.6	32.7	195.3	379.9
4	32.3	20.7	21.5	23.4	24.5	5.4	154.7	39.3	14.5	69.5	74.8	2.8	4.8	11.6	14.8
5	2.0	1.9	1.2	2.6	1.9	0.6	290.7	142.0	44.8	159.1	123.8	84.1	148.6	4443.4	7592.1
6	32.7	65.0	39.7	44.3	45.4	13.9	80.7	207.7	11.0	99.8	99.7	2.2	2.5	4.8	7.6
7	28.3	51.7	36.7	33.7	37.6	10.0	250.3	209.3	183.0	214.2	33.9	5.7	8.8	15.2	31.2
8	23.6	200.3	30.7	15.4	67.5	88.8	269.0	343.0	13.7	208.6	172.8	3.1	11.4	4.6	48.2
9	3.1	32.7	14.0	9.6	14.8	12.7	400.0	400.0	144.7	314.9	147.4	21.2	128.0	142.8	4096.0
10	5.1	24.7	10.5	22.2	15.6	9.4	93.3	158.0	9.6	87.0	74.4	5.6	18.4	35.7	363.6
11	2.9	4.5	2.8	4.9	3.8	1.1	297.0	400.0	310.0	335.7	56.1	89.1	102.4	2364.8	3531.5
12	283.0	400.0	173.0	170.7	256.7	109.0	363.7	315.7	268.3	315.9	47.7	1.2	1.3	0.5	0.5
13	75.7	128.7	87.0	170.7	115.5	43.3	218.3	346.7	127.7	230.9	110.0	2.0	2.9	1.7	3.8
14	9.8	16.1	12.1	13.0	12.7	2.6	310.3	344.3	8.2	221.0	185.0	17.4	31.7	136.3	323.1
15	22.7	84.3	135.3	29.7	68.0	52.7	23.7	105.3	5.3	44.8	53.3	0.7	1.0	1.0	4.6
16	69.0	88.7	77.3	28.0	65.8	26.4	33.7	40.0	8.2	27.3	16.8	0.4	0.5	0.6	0.7
17	31.3	82.3	39.0	45.3	49.5	22.6	191.7	200.0	206.3	199.3	7.4	4.0	6.1	8.1	19.5
18	18.9	65.3	82.3	60.0	56.6	26.9	334.3	400.0	82.3	272.2	167.7	4.8	17.7	8.5	93.6
DXR	0.170	0.078	0.078	0.078	0.101	0.046	10.0	10.0	0.4	6.8	5.5	67.4	58.8	66736.4	34602.1

DXR: Doxorubicin; Ca9-22, derived from gingival tissue; HSC-2, HSC-3 and HSC-4, derived from tongue. Compounds **1-18** are shown in bold.

Hungary) (23), was optimized by CORINA Classic (Molecular Networks GmbH, Germany) with forcefield calculations (amber-10: EHT) in Molecular Operating Environment (MOE) version 2018.0101 (Chemical Computing Group Inc., Quebec, Canada) (24). The number of structural descriptors calculated from MOE and Dragon (Dragon 7 version 7.0.2 (Kode srl., Pisa, Italy) (25) was 354 and 5,255, respectively. Among them, the number of descriptors used for analysis was 287 and 2,830 (total 3,117), respectively.

Statistical analysis. The CC_{50} values were expressed as mean±S.D. of triplicate assays. The relation among cytotoxicity, tumor-specificity index and chemical descriptors was investigated using simple regression analyses by JMP Pro version 14.1.0 (SAS Institute Inc., Cary, NC, USA). The significance level was set at $p<0.05$.

Results

Cytotoxicity and tumor-specificity. Among eighteen synthetic 2-styrylchromones, [**5**] showed the highest cytotoxicity against four OSCC cell lines (mean CC_{50}=1.9 μM) (B in Table I), followed by [**11**] (3.8) > [**3**] (10.6) > [**14**] (12.7) > [**9**] (14.8) > [**10**] (15.6) > [**2**] (19.8) > [**4**] (24.5) > [**7**] (37.6) > [**1**] (37.7) > [**6**] (45.4) > [**17**] (49.5) > [**18**] (56.6) > [**16**] (65.8) > [**8**] (67.5) > [**15**] (68.0) > [**13**] (115.5) > [**12**] (256.7 μM). On the other hand, [**16**] showed the highest cytotoxicity against three normal oral mesenchymal cells (mean CC_{50}=27.3 μM) (D in Table I), followed by [**15**] (44.8) > [**4**] (69.5) > [**1**] (79.2) > [**10**] (87.0) > [**6**] (99.8) > [**5**] (159.1) > [**2**] (175.6) > [**17**] (199.3) > [**8**] (208.6) > [**7**] (214.2) > [**3**] (218.1) > [**14**] (221.0) > [**13**] (230.9) > [**18**] (272.2) > [**9**] (314.9) > [**12**] (315.9) > [**11**] (335.7 μM) (Table I). When tumor-specificity (TS) was calculated by the ratio of mean CC_{50} for non-malignant (normal oral cells) to that of malignant (OSCC cells) (D/B in Table I), [**11**] showed the highest TS value (89.1), followed by [**5**] (84.1) > [**9**] (21.2) > [**3**] (20.6) > [**14**] (17.4) > [**2**] (8.9) > [**7**] (5.7) > [**10**] (5.6) > [**18**] (4.8) > [**17**] (4.0) > [**8**] (3.1) > [**4**] (2.8) > [**6**] (2.2) > [**1**] (2.1) > [**13**] (2.0) > [**12**] (1.2) > [**15**] (0.7) > [**16**] (0.4). [**5**] also showed the highest PSE value [(D/B^2) ×100 in Table I] (4443.4), followed by [**11**] (2364.8) > [**3**] (195.3) > [**9**] (142.8) > [**14**] (136.3) > [**2**] (44.9) > [**10**] (35.7) > [**7**] (15.2) > [**4**] (11.6) > [**18**] (8.5) > [**17**] (8.1) > [**1**] (5.6) > [**6**] (4.8) > [**8**] (4.6) > [**13**] (1.7) > [**15**] (1.0) > [**16**] (0.6) > [**12**] (0.5).

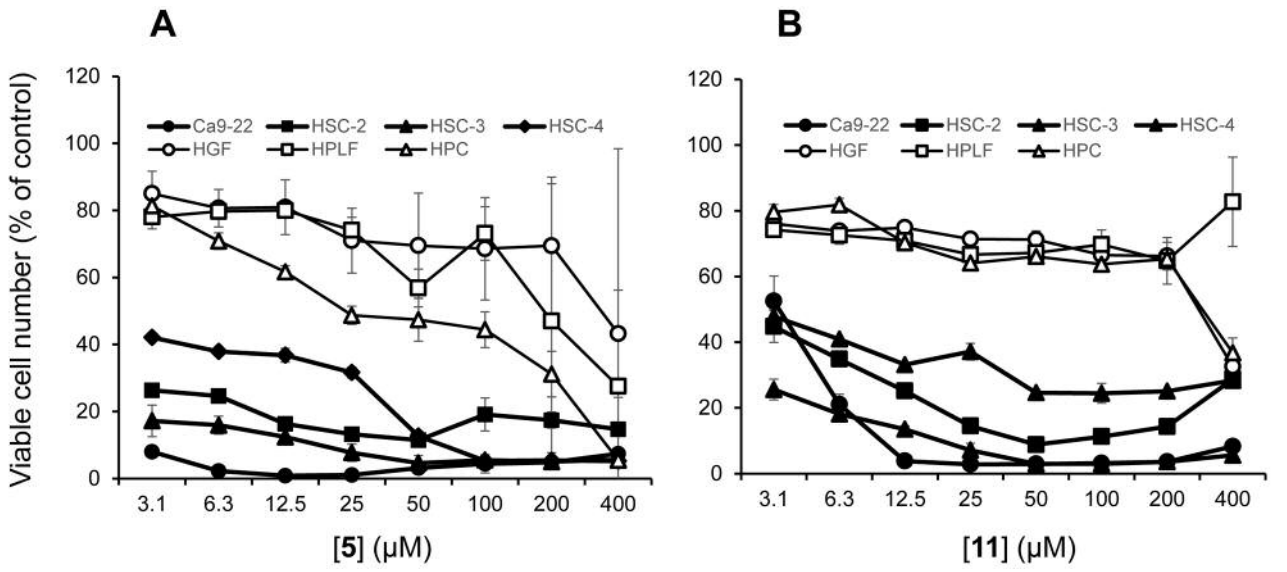

Figure 2. *Cytotoxicity of compounds [**5, 11**] against four human OSCC cell lines, Ca9-22 (●), HSC-2 (■), HSC-3 (▲) and HSC-4) (◆), and three human normal mesenchymal oral cells, HGF (○), HPLF (□) and HPC (△). Cells were incubated for 48 h without (control) or with the indicated concentrations of [**5**] (A) or [**11**] (B), and cell viability was determined by the MTT method, and expressed as a percentage to that of control. Each value represents the mean±S.D. of triplicate assays.*

The prominent TS and PSE values of [**5, 11**] were not changed when Ca9-22 and HGF, both derived from gingival tissues, were used as target cell: TS=148.6, 102.4 (C/A) and PSE=7592.1, 3531.5 [$(C/A^2) \times 100$ in Table I], respectively. Dose-response curves (Figure 2A and 2B) showed clearly that all OSCC cells (Ca9-22, HSC-2, HSC-3, HSC-4) were more sensitive to [**5, 11**] than normal oral cells (HGF, HPLF, HPC). Cell-cycle analysis demonstrated that both [**5, 11**] accumulated the $subG_1$ and G_2/M phase cells, suggesting the induction of apoptosis (Figure 3).

Computational analysis. QSAR analysis of cytotoxicity and tumor-specificity of eighteen 2-styrylchromone derivatives [**1-18**] were next performed. Since significant correlation ($p<0.05$) was found between cytotoxicity against tumor and normal cells, and TS with 139, 472 and 67 chemical descriptors (data not shown), top six chemical descriptors were chosen for QSAR analysis (Figures 4, 5 and 6; Table II).

Cytotoxicity of eighteen 2-styrylchromones against human OSCC cell lines was negatively correlated with J_D (topological shape) ($r^2=0.555$, $p=0.0004$), balabanJ (topological shape) ($r^2=0.533$, $p=0.0006$), CATS2D_09_AL (hydrogen-bond acceptor and lipophilicity) ($r^2=0.486$, $p=0.0013$), RDF085p (3D shape and polarizability) ($r^2=0.471$, $p=0.0017$), L2s (3D shape, size and electric state) ($r^2=0.468$, $p=0.0017$) and H2u (3D shape) ($r^2=0.452$, $p=0.0022$) (Figure 4).

Cytotoxicity of eighteen 2-styrylchromones against normal oral cells was positively correlated with descriptors H2v (3D shape and size) ($r^2=0.537$, $p=0.0005$), H2p (3D shape and polarizability) ($r^2=0.502$, $p=0.0010$), TDB09r (3D shape and size) ($r^2=0.492$, $p=0.0012$), TDB07m (3D shape and size)($r^2=0.484$, $p=0.0013$) and Mor08m (3D shape and size) ($r^2=0.478$, $p=0.0015$), but negatively correlated with Mor11e (3D shape and electric state) ($r^2=0.470$, $p=0.0017$) (Figure 5).

TS of eighteen 2-styrylchromones was positively correlated with H8i (3D shape and ionization potential) ($r^2=0.516$, $p=0.0008$), HATS5e (3D shape, size and electric state) ($r^2=0.462$, $p=0.0019$) and Ks (3D shape, size and electric state) ($r^2=0.455$, $p=0.0021$), but negatively correlated with J_Dz(m) (topological shape and size) ($r^2=0.504$, $p=0.0010$), P2s (3D shape, size and electric state) ($r^2=0.457$, $p=0.0021$) and balabanJ (topological shape) ($r^2=0.431$, $p=0.0031$) (Figure 6).

Discussion

The present study demonstrated that two compounds: 2-[(1*E*)-2-(4-methoxyphenyl)ethenyl]-4*H*-1-benzopyran-4-one [**5**] and 6-methoxy-2-[(1*E*)-2-(4-methoxyphenyl)ethenyl]-4*H*-1-benzopyran-4-one [**11**], showed comparable tumor-specificity with doxorubicin, an anthracycline anticancer drug (26, 27) (TS=84.1, 89.1 *vs*. 67.4 in D/B; 148.6, 102.4 *vs*. 58.8 in C/A, Table I). However, [**5, 11**] showed much lower PSE values compared to doxorubicin, possibly due to much lower cytotoxicity against OSCC cell lines (Table I). Structure–activity relationship suggests the importance of having OCH_3 group in R^4 position in [**5**], and two OCH_3

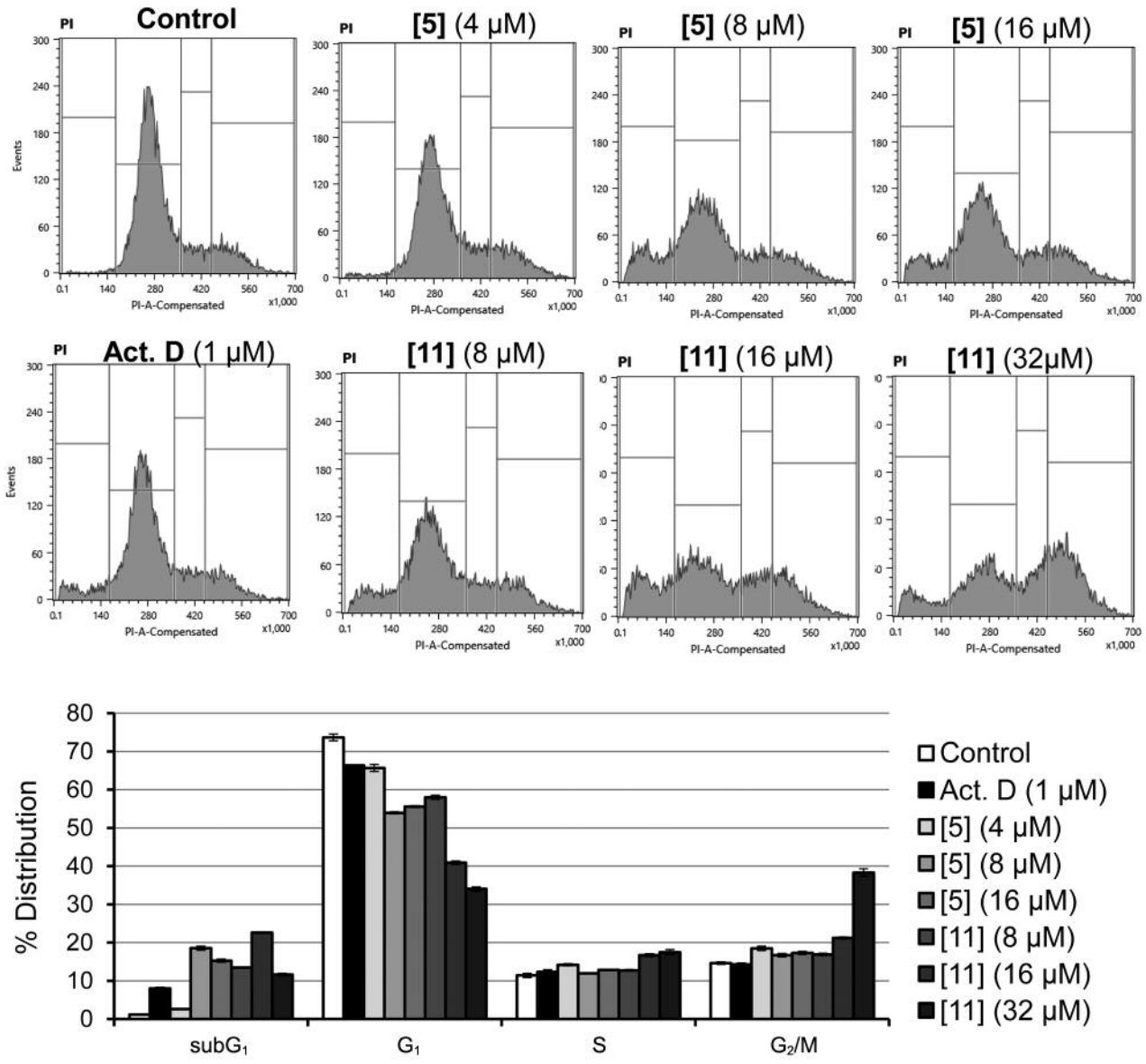

Figure 3. *Effect of [**5, 11**] on cell-cycle distribution in HSC-2 cells. HSC-2 cells were incubated for 24 h with the indicated concentrations of [**5**], [**11**] or 1 μM actinomycin D (Act D) as a positive control and then assessed for cell-cycle distribution by a cell sorter.*

groups in R^1 and R^4 positions in [**11**]. However, [**12**] having three OCH_3 groups in R^1, R^3 and R^4 positions, showed significantly reduced tumor-specificity (Figure 1, Table I). This may be explained by the dependence of tumor-specificity on molecular shape, since the cytotoxicity of eighteen 2-styrylchromones against tumor cell lines was significantly (p<0.002) correlated with topological and 3D shape, size, hydrogen-bond acceptor, lipophilicity, polarizability and electric state (Figure 4), and tumor-specificity was also significantly (p<0.004) correlated with topological and 3D shape, size, ionization potential and electric state (Figure 6).

The present study also demonstrated that both [**5, 11**] produced $subG_1$ cell population (a marker of apoptosis) and induced mitotic arrest (Figure 3). This is consistent with a previous report that 4'-methoxy-2-styrylchromone stabilized microtubules in a manner similar to paclitaxel, inducing abnormal mitotic spindles characterized by the formation of a monopolar structure, leading to mitotic arrest in human breast adenocarcinoma MCF-7 and lung

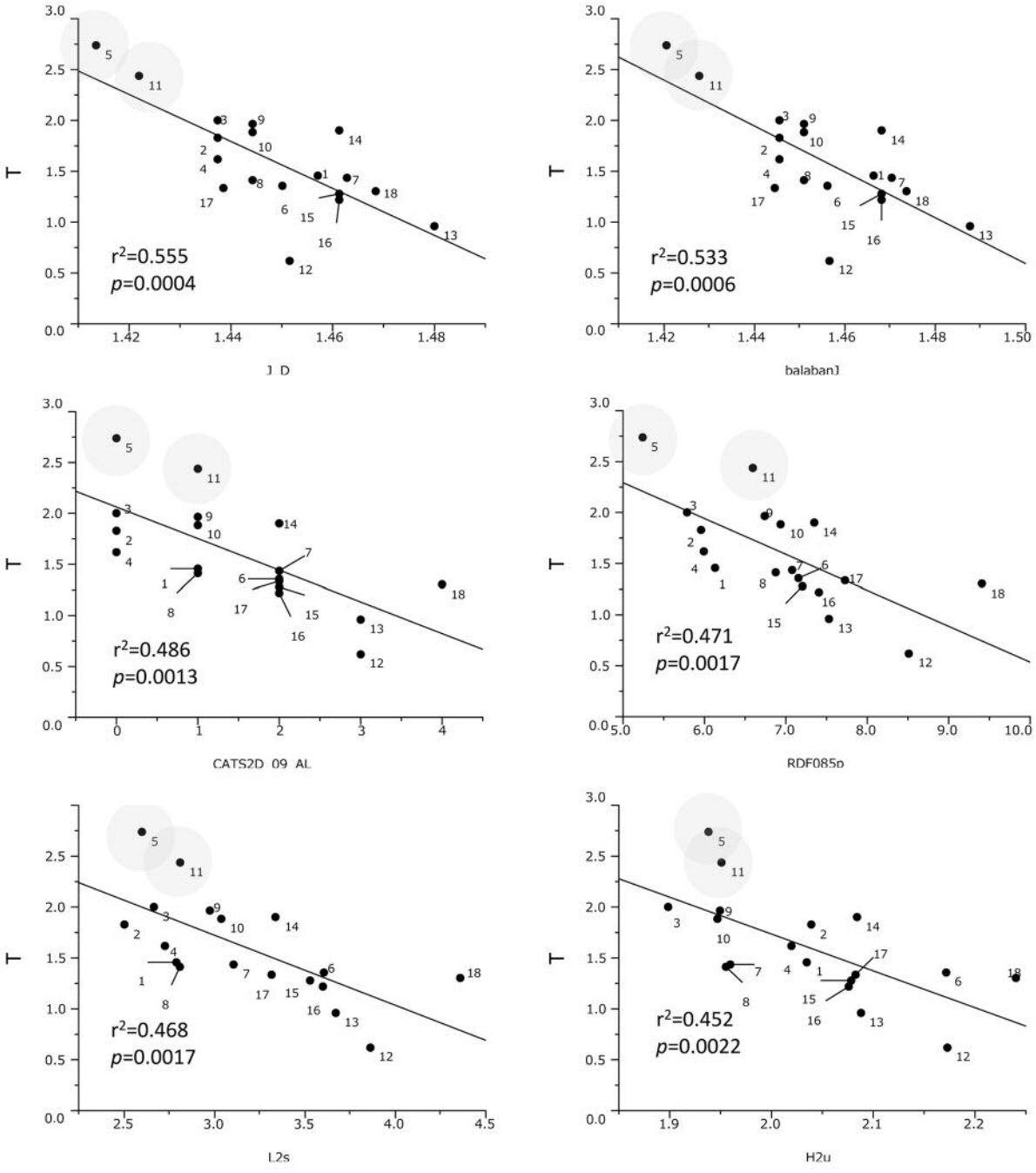

Figure 4. *Top six chemical descriptors that showed higher correlation with cytotoxicity of eighteen 2-styrylchromone derivatives [**1-18**] against OSCC cells. The mean negative log CC_{50} values (T) against tumor cells were plotted. CC_{50}: concentration of compound that reduced the viable cell number by 50%. Top six chemical descriptors were: J_D (topological shape), balabanJ (topological shape), CATS2D_09_AL (hydrogen-bond acceptor and lipophilicity), RDF085p (3D shape and polarizability), L2s (3D shape,size and electric state) andH2u (3D shape).*

adenocarcinoma NCI-H460 cell lines (16). It should be noted that both [**5, 11**] induced apoptosis (subG_1 population) of HSC-2 cells more potently than actinomycin D, positive control of apoptosis (28). Induction of both apoptosis and G_2+M arrest may further potentiate the antitumor potential.

We previously reported that [**5**] (identical with the compound 3 in (18)) induced internucleosomal DNA fragmentation and

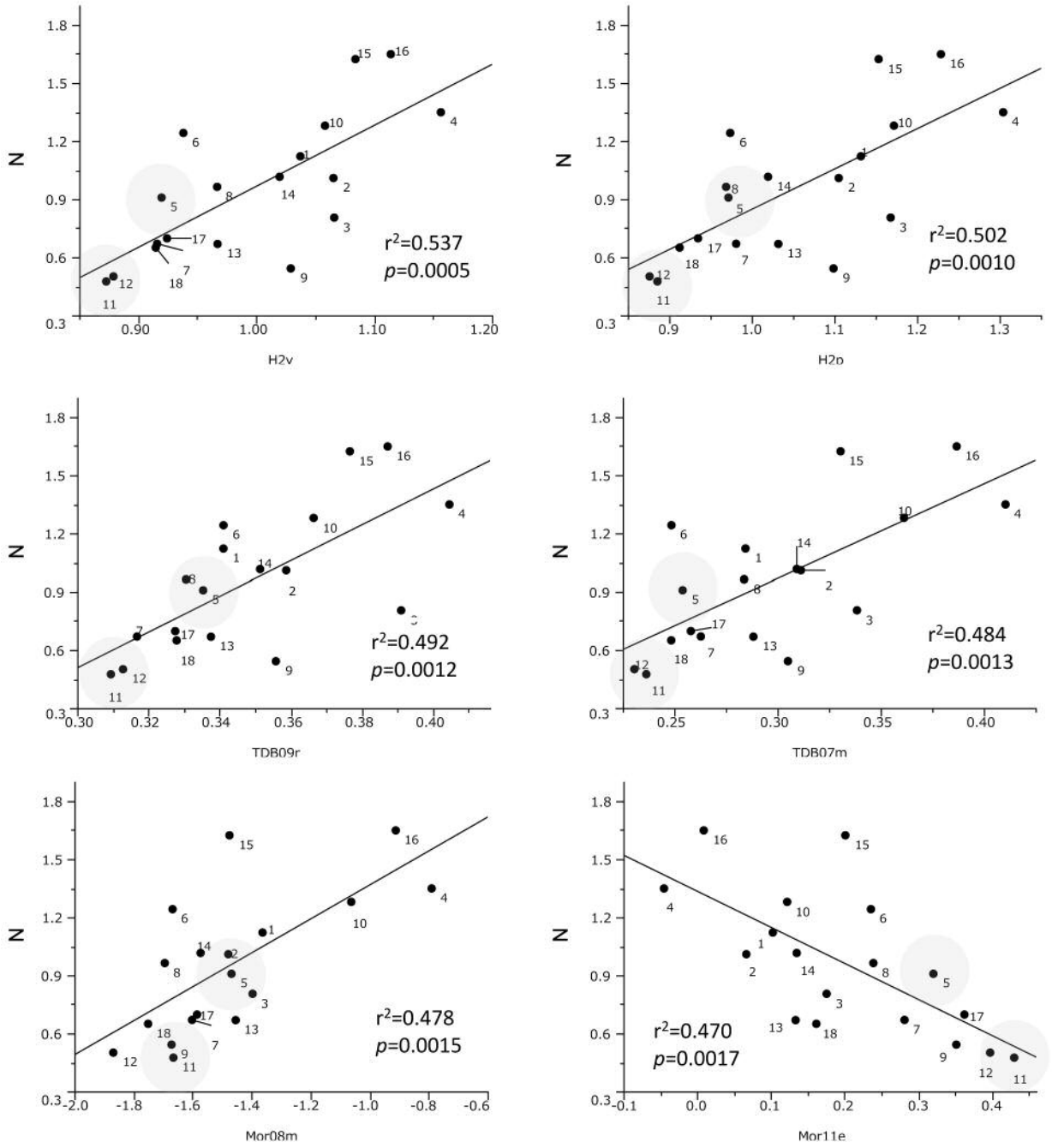

Figure 5. *Top six chemical descriptors that showed higher correlation with cytotoxicity of eighteen 2-styrylchromone derivatives [**1-18**] against normal oral cells. The mean negative log CC_{50} values (N) against normal cells were plotted. Top six chemical descriptors were: H2v (3D shape and size), H2p (3D shape and polarizability), TDB09r (3D shape and size), TDB07m (3D shape and size), Mor08m (3D shape and size) and Mor11e (3D shape and electric state).*

activation of caspase-3, 8 and 9 in human promyelocytic leukemia HL-60 cells, but produced large DNA fragment (assessed on agarose gel electrophoresis) in HSC-2 cells (18). Lipophilic property of [**5**] (logP=2.6) (18) may facilitate its intracellular entry. As far as we know, there are only two papers about the antitumor potential of 4'-methoxy-2-styrylchromone including ours (16, 18). Compound [**5, 11**] can, thus, be a lead compound for designing a new type of anticancer drug.

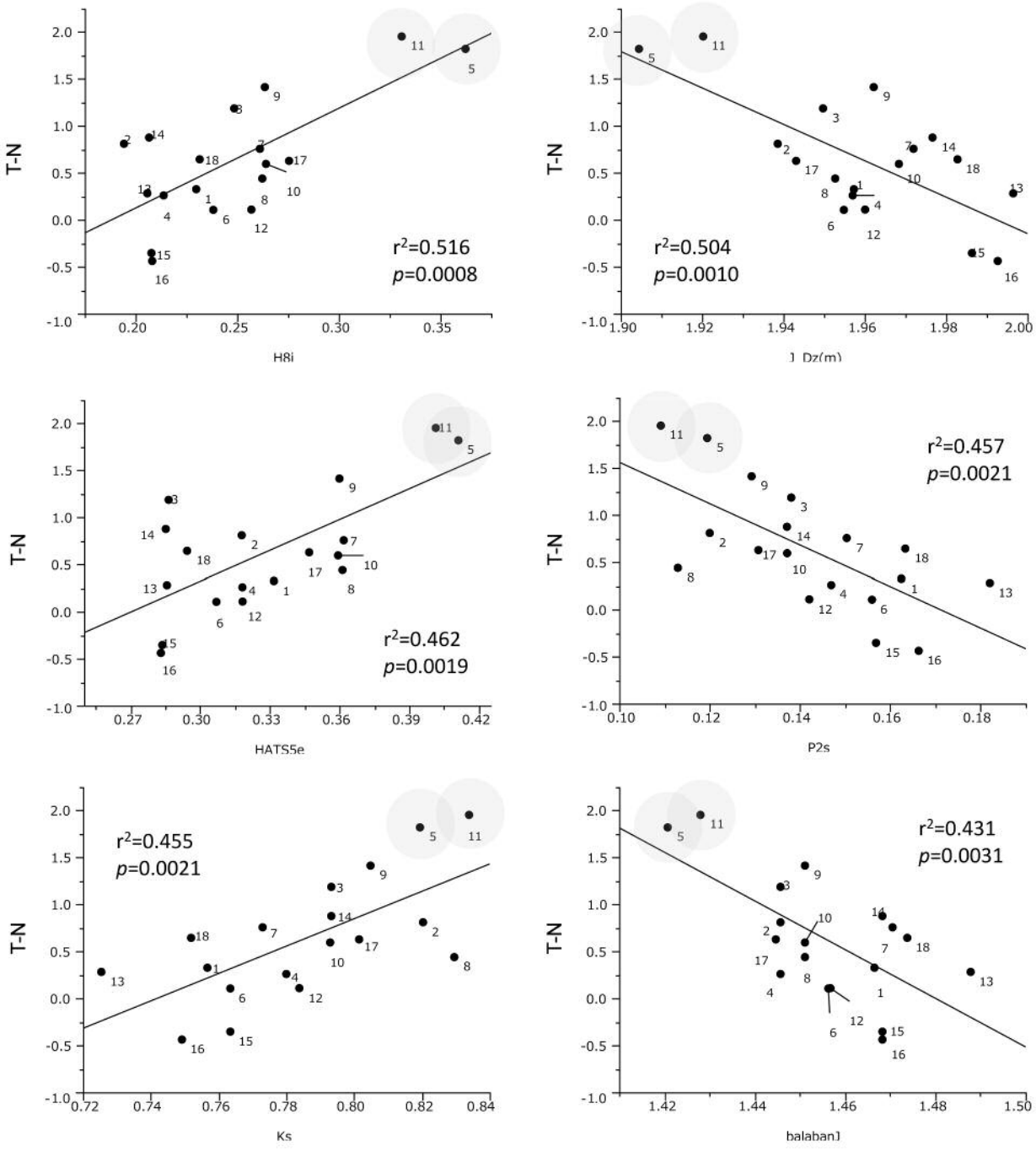

Figure 6. *Top six chemical descriptors that showed higher correlation with tumor-specificity of eighteen 2-styrylchromone derivatives [**1-18**]. The mean negative logTS values (T-N) were plotted. Top six chemical descriptors were: H8i (3D shape and ionization potential), J_Dz(m) (topological shape and size), HATS5e (3D shape, size and electric state), P2s (3D shape, size and electric state), Ks (3D shape, size and electric state) and balabanJ (topological shape).*

We recently found that the tumor-specificity of 3-(*N*-cyclicamino)chromone derivatives (29), 2-(*N*-cyclicamino) chromone (21), pyrano[4,3-*b*]chromones (30) and furo[2,3-*b*]chromones (31) was also well correlated with descriptors that reflect the molecular shape. The next step of our research is to estimate the structure that should show higher tumor-specificity based on the accumulated QSAR data base, and then synthesize such compound for the

Table II. *Properties of descriptors that significantly correlated with cytotoxicity against tumor cells (T) and normal cells (N), and tumor-specificity (T-N).*

	Descriptor	Source	Meaning	Explanation
T	J_D	Dragon	Topological shape	Balaban-like index from topological distance matrix (Balaban distance connectivity index)
	balabanJ	MOE	Topological shape	Balaban's connectivity topological index
	CATS2D_09_AL	Dragon	Hydrogen-bond acceptor and lipophilicity	CATS2D Acceptor-Lipophilic at lag 09
	RDF085p	Dragon	3D shape and polarizability	Radial Distribution Function - 085/weighted by polarizability
	L2s	Dragon	3D shape, size and electric state	2nd component size directional WHIM index/weighted by I-state
	H2u	Dragon	3D shape	H autocorrelation of lag 2/unweighted
N	H2v	Dragon	3D shape and size	H autocorrelation of lag 2/weighted by van der Waals volume
	H2p	Dragon	3D shape and polarizability	H autocorrelation of lag 2/weighted by polarizability
	TDB09r	Dragon	3D shape and size	3D Topological distance based descriptors - lag 9 weighted by covalent radius
	TDB07m	Dragon	3D shape and size	3D Topological distance based descriptors - lag 7 weighted by mass
	Mor08m	Dragon	3D shape and size	signal 08/weighted by mass
	Mor11e	Dragon	3D shape and electric state	signal 11/weighted by Sanderson electronegativity
T-N	H8i	Dragon	3D shape and ionization potential	H autocorrelation of lag 8/weighted by ionization potential
	J_Dz(m)	Dragon	Topological shape and size	Balaban-like index from Barysz matrix weighted by mass
	HATS5e	Dragon	3D shape, size and electric state	leverage-weighted autocorrelation of lag 5/weighted by Sanderson electronegativity
	P2s	Dragon	3D shape, size and electric state	2nd component shape directional WHIM index/weighted by I-state
	Ks	Dragon	3D shape, size and electric state	K global shape index/weighted by I-state
	balabanJ	MOE	Topological shape	Balaban's connectivity topological index

confirmation of tumor-specificity. Repeating this process may make it possible to manufacture clinically applicable compounds. The other direction of approach is to synthesize the ^{13}C-labeled compound to monitor its intracellular distribution for the identification of target molecule.

Conflicts of Interest

The Authors confirm that there are no known conflicts of interest associated with this publication and there has been no significant financial support for this work that could have influenced its outcome.

Authors' Contributions

Y.U. and J.N. performed the QSAR analysis. HX.S. and H.S. performed the cytotoxicity assay. K.B., A.T. and M.T. performed the cell cycle analysis. S.E., K.T. and Y.S. synthesized 18 test compounds. Y.U., H.S. and Y.S. authored or reviewed drafts of the article.

Acknowledgements

This work was partially supported by KAKENHI from the Japan Society for the Promotion of Science (JSPS) (15K08111, 16K11519).

References

1 Sakagami H: Biological activities and possible dental application of three major groups of polyphenols. J Pharmacol Sci 126: 92-106, 2014. PMID: 25263279. DOI: 10.1254/jphs.14r04cr

2 Sugita Y, Takao K, Uesawa Y and Sakagami H: Search for new type of anticancer drugs with high tumor-specificity and less keratinocyte toxicity (Review). Anticancer Res *37(11):* 5919-5924, 2017. PMID: 29061770. DOI: 10.21873/anticanres.12038

3 Sakagami H, Watanabe T, Hoshino T, Suda N, Mori K, Yasui T, Yamauchi N, Kashiwagi H, Gomi T, Oizumi T, Nagai J, Uesawa Y, Takao K and Sugita Y: Recent progress of basic studies of natural products and their dental application. Medicines (Basel). *6(1):* 4, 2019. PMID: 30585249. DOI: 10.3390/medicines 6010004

4 Sousa JL, Proença C, Freitas M, Fernandes E and Silva AM: New polyhydroxylated flavon-3-ols and 3-hydroxy-2-styrylchromones: synthesis and ROS/RNS scavenging activities. Eur J Med Chem *119:* 250-259, 2016. PMID: 27213247. DOI: 10.1016/j.ejmech.2016.04.057.

5 Gomes A, Fernandes E, Silva AM, Santos CM, Pinto DC, Cavaleiro JA and Lima JL: 2-Styrylchromones: novel strong scavengers of reactive oxygen and nitrogen species. Bioorg Med Chem *15(18):* 6027-6036, 2007. PMID: 17624791. DOI: 10.1016/j.bmc.2007.06.046

6 Gomes A, Capela JP, Ribeiro D, Freitas M, Silva AM, Pinto DC, Santos CM, Cavaleiro JA, Lima JL and Fernandes E: Inhibition of NF-kB activation and cytokines production in THP-1 monocytes by

2-styrylchromones. Med Chem *11(6):* 560-566, 2015. PMID: 25665653. DOI: 10.2174/1573406411666150209114702

7 Fernandes E, Carvalho M, Carvalho F, Silva AM, Santos CM, Pinto DC, Cavaleiro JA and de Lourdes Bastos M: Hepatoprotective activity of polyhydroxylated 2-styrylchromones against *tert*-butylhydroperoxide induced toxicity in freshly isolated rat hepatocytes. Arch Toxicol *77(9):* 500-505, 2003. PMID: 12879211. DOI: 10.1007/s00204-003-0480-9

8 Jung HJ, Jung HA, Min BS and Choi JS: Anticholinesterase and β-site amyloid precursor protein cleaving enzyme 1 inhibitory compounds from the heartwood of *Juniperus chinensis*. Chem Pharm Bull (Tokyo) *63(11):* 955-960, 2015. PMID: 26521861. DOI: 10.1248/cpb.c15-00504

9 Ono M, Maya Y, Haratake M and Nakayama M: Synthesis and characterization of styrylchromone derivatives as beta-amyloid imaging agents. Bioorg Med Chem *15(1):* 444-450, 2007. PMID: 17035032. DOI: 10.1016/j.bmc.2006.09.044

10 Yoon JS, Lee MK, Sung SH and Kim YC: Neuroprotective 2-(2-phenylethyl)chromones of *Imperata cylindrica*. J Nat Prod *69(2):* 290-291, 2006. PMID: 16499335. DOI: 10.1021/np0503808

11 Chaniad P, Wattanapiromsakul C, Pianwanit S and Tewtrakul S: Anti-HIV-1 integrase compounds from *Dioscorea bulbifera* and molecular docking study. Pharm Biol *54(6):* 1077-1085, 2016. PMID: 26864337. DOI: 10.3109/13880209.2015.1103272

12 Rocha-Pereira J, Cunha R, Pinto DC, Silva AM and Nascimento MS: (E)-2-Styrylchromones as potential anti-norovirus agents. Bioorg Med Chem *18(12)*: 4195-4201, 2010. PMID: 20554208. DOI: 10.1016/j.bmc.2010.05.006

13 Conti C, Mastromarino P, Goldoni P, Portalone G and Desideri N: Synthesis and anti-rhinovirus properties of fluoro-substituted flavonoids. Antivir Chem Chemother *16(4):* 267-276, 2005. PMID: 16130524. DOI: 10.1177/095632020501600406

14 Desideri N, Mastromarino P and Conti C: Synthesis and evaluation of antirhinovirus activity of 3-hydroxy and 3-methoxy 2-styrylchromones. Antivir Chem Chemother *14(4):* 195-203, 2003. PMID: 14582848. DOI: 10.1177/095632020301400404

15 Shaw AY, Chang CY, Liau HH, Lu PJ, Chen HL, Yang CN and Li HY: Synthesis of 2-styrylchromones as a novel class of antiproliferative agents targeting carcinoma cells. Eur J Med Chem *44(6):* 2552-2562, 2009. PMID: 19246129. DOI: 10.1016/j.ejmech.2009.01.034

16 Marinho J, Pedro M, Pinto DC, Silva AM, Cavaleiro JA, Sunkel CE and Nascimento MS: 4'-Methoxy-2-styrylchromone a novel microtubule-stabilizing antimitotic agent. Biochem Pharmacol *75(4):* 826-835, 2008. PMID: 18036572. DOI: 10.1016/j.bcp.2007.10.014

17 Peixoto F, Barros AI and Silva AM: Interactions of a new 2-styrylchromone with mitochondrial oxidative phosphorylation. J Biochem Mol Toxicol *16(5):* 220-226, 2002. PMID: 12439863. DOI: 10.1002/jbt.10042

18 Momoi K, Sugita Y, Ishihara M, Satoh K, Kikuchi H, Hashimoto K, Yokoe I, Nishikawa H, Fujisawa S and Sakagami H: Cytotoxic activity of styrylchromones against human tumor cell lines. In Vivo *19(1):* 157-163, 2005. PMID: 15796168.

19 Takao K, Endo S, Nagai J, Kamauchi H, Takemura Y, Uesawa Y and Sugita Y: 2-Styrylchromone derivatives as potent and selective monoamine oxidase B inhibitors. Bioorg Chem *92*: 103285, 2019. PMID: 31561103. DOI: 10.1016/j.bioorg.2019.103285

20 Sakagami H, Shimada C, Kanda Y, Amano O, Sugimoto M, Ota S, Soga T, Tomita M, Sato A, Tanuma S, Takao K and Sugita Y: Effects of 3-styrylchromones on metabolic profiles and cell death in oral squamous cell carcinoma cells. Toxocol Rep *2:* 1281-1290, 2015. PMID: 28962471. DOI: 10.1016/j.toxrep.2015.09.009

21 Shi H, Nagai J, Sakatsume T, Bandow K, Okudaira N, Sakagami H, Tomomura M, Tomomura A, Uesawa Y, Takao K and Sugita Y: Quantitative structure–cytotoxicity relationship of 2-(*N*-cyclicamino)chromone derivatives. Anticancer Res *38(7):* 3897-3906, 2018. PMID: 29970510. DOI: 10.21873/anticanres.12674

22 Horikoshi M, Kimura Y, Nagura H, Ono T and Ito H: A new human cell line derived from human carcinoma of the gingiva. I. Its establishment and morphological studies. Jpn J Oral Maxillofac Surg *20:* 100-106, 1974. PMID: 4549822. DOI: 10.5794/jjoms.20.100

23 MarvinSketch 18.10.0. Available at: http://www.chemaxon.com. Last accessed on 16th October 2019.

24 MOE2019.0101, Chemical Computing Group. Available at: https://www.chemcomp.com/Products.htm. Last accessed on 16th October 2019.

25 Dragon 7. Available at: https://chm.kode-solutions.net/products_dragon_descriptors.php. Last accessed on 16th October 2019.

26 Piska K, Koczurkiewicz P, Bucki A, Wójcik-Pszczoła K, Kołaczkowski M and Pękala E: Metabolic carbonyl reduction of anthracyclines – role in cardiotoxicity and cancer resistance. Reducing enzymes as putative targets for novel cardioprotective and chemosensitizing agents. Invest New Drugs *35(3):* 375-385, 2017. PMID: 28283780. DOI: 10.1007/s10637-017-0443-2

27 Mordente A, Meucci E, Martorana GE, Tavian D and Silvestrini A: Topoisomerases and anthracyclines: recent advances and perspectives in anticancer therapy and prevention of cardiotoxicity. Curr Med Chem *24(15):* 1607-1626, 2017. PMID: 27978799. DOI: 10.2174/0929867323666161214120355

28 Sameni HR, Javadinia SS, Safari M, Tabrizi Amjad MH, Khanmohammadi N, Parsaie H and Zarbakhsh S: Effect of quercetin on the number of blastomeres, zona pellucida thickness, and hatching rate of mouse embryos exposed to actinomycin D: An experimental study. Int J Reprod Biomed (Yazd) *16(2):* 101-108, 2018. PMID: 29675494.

29 Shi H, Nagai J, Sakatsume T, Bandow K, Okudaira N, Uesawa Y, Sakagami H, Tomomura M, Tomomura A, Takao K and Sugita Y: Quantitative structure-cytotoxicity relationship of 3-(*N*-cyclicamino)chromone derivatives. Anticancer Res *38(8):* 4459-4467, 2018. PMID: 30061210. DOI: 10.21873/anticanres.12748

30 Nagai J, Shi H, Kubota Y, Bandow K, Okudaira N, Uesawa Y, Sakagami H, Tomomura M, Tomomura A, Takao K and Sugita Y: Quantitative structure-cytotoxicity relationship of pyrano[4,3-*b*]chromones. Anticancer Res *38(8):* 4449-4457, 2018. PMID: 30061209. DOI: 10.21873/anticanres.12747

31 Uesawa Y, Sakagami H, Shi H, Hirose M, Takao K and Sugita Y: Quantitative structure-cytotoxicity relationship of furo[2,3-*b*]chromones. Anticancer Res *38(6):* 3283-3290, 2018. PMID: 29848675. DOI: 10.21873/anticanres.12593

Received November 12, 2019
Revised November 16, 2019
Accepted November 20, 2019